

SKYRMION STARS

RACHID OUYED¹ AND MALCOLM BUTLER

Department of Astronomy and Physics, Saint Mary's University, Halifax, Nova Scotia, B3H 3C3, Canada; rouyed@ap.stmarys.ca, mbutler@ap.stmarys.ca

Received 1998 October 5; accepted 1999 April 12

ABSTRACT

With a newly derived equation of state (EOS) of dense matter, we construct zero-temperature compact-star models in hydrostatic equilibrium, for central densities $1.0 \leq \rho_c/\rho_N \leq 10.0$ ($\rho_N = 2.575 \times 10^{14} \text{ g cm}^{-3}$ is the nuclear saturation density). Based on Skyrme's concept of baryons as solitons (of finite extent) in the meson field, the new EOS represents a fluid of Skyrmions coupled to a dilaton field (associated with the glueball of quantum chromodynamics) and a vector meson field (coupled to the baryon number). We find stable configurations to exist for $\rho_c/\rho_N \leq 5.0$, and they are mostly fluid (the Skyrmion fluid); we thus name them "Skyrmion stars." The outer region of the star (the crust, for densities below the nuclear saturation density) is constructed using the EOS of Baym, Pethick, and Sutherland and accounts on average for 15% of the total mass of the star. Their masses and radii are $0.5 \leq M/M_\odot \leq 2.95$ and $11.0 \text{ km} \leq R \leq 15.3 \text{ km}$, respectively. The new EOS describes a fluid of Skyrmions with a unique behavior at high densities. The Skyrmions shrink as the density increases, allowing for a high compression of matter near the core of the star and thus greater gravitational binding energy. The heaviest stars, which can then withstand greater centrifugal forces, are expected to rotate the fastest in our model. Much of this interesting behavior is inherent in the glueball potential, with its negative contribution to the pressure acting to bind the system; the Skyrmion responds in a nonlinear fashion by shrinking (a result of Skyrmions having structure). Skyrmion stars are fundamentally different from quark stars; the quark degrees of freedom are integrated out, leaving only meson degrees of freedom. Furthermore, unlike boson/soliton stars where the soliton describes the global structure of the star, Skyrmion stars can be looked at as being made of fermionic soliton objects.

Subject headings: dense matter — elementary particles — equation of state — stars: interiors — stars: rotation

1. INTRODUCTION

The role that the equation of state (EOS) of dense matter plays in astrophysics has long been the subject of detailed theoretical and numerical investigations (Glendenning 1989; Weber & Weigel 1989; Lattimer & Swesty 1991; Brown & Bethe 1994; Pethick et al. 1995; Baldo, Bombaci, & Burgio 1997; Prakash et al. 1997; Akmal, Pandharipande, & Ravenhall 1998; Shen et al. 1998; to cite only few). These investigations have largely been motivated by the fact that the behavior of matter at nuclear densities and above is not yet well constrained by experiment or observation. Matter in the cores of neutron stars possesses densities ranging from a few times the density of normal nuclear matter to about an order of magnitude higher, depending on the star mass. At present, hundreds of pulsars are known, and the discovery of new ones is rather frequent. This is accompanied by an impressive growth rate of the body of observed pulsar data, which one can use to confront the many theoretical/numerical EOSs so far proposed.

In this paper, we shall apply a new EOS to the study of the structure of compact stars. The new EOS used is based on Skyrme's concept of baryons as solitons. Skyrme (1962), by constructing a model of pion interactions consisting of a conventional model of weak meson interactions, found that in his model the meson fields contained points in space where there was a "topological knot." These structures turned out to be "topological solitons" (solitons of finite extent whose number is always conserved), which Skyrme

identified as baryons. Our interest in such a model arose from its recent revival due to its possible connection to quantum chromodynamics (QCD). It appears that a model of nuclei and nuclear matter based on Skyrmions might be better related to more fundamental theories of matter. This is especially appealing because of its mathematical simplicity, compared with the difficulty of solving QCD explicitly.

Our goal is then twofold: to check to see if the EOS derived from a current variation of the Skyrme model can reproduce the properties of observed compact models and, if the EOS fails in this first attempt, to put constraints on the Skyrme model on the basis of that failure. In § 2, we introduce the reader to the basic concept of Skyrmions as topological solitons and their identification as single baryons. The recent revival of the Skyrme model and its plausible derivation from fundamental QCD is presented. In § 3, we explain how Skyrmions can constitute a fluid based on a mean field approach and develop the corresponding EOS. We go on in § 4 to construct the corresponding models of compact stars, which we call "Skyrmion stars," and compare those models with observations. We conclude in § 5.

2. SKYRMIONS AND QCD

QCD is the fundamental theory of strong interactions. It describes the interactions between quarks, which in turn should imply the interactions between nucleons (composed of quarks). Unfortunately, this inference is not arrived at easily and to date has not been derived. Instead, we must rely on either effective field theories or models to bind quarks into nucleons (we refer the interested reader to Bhaduri 1988).

¹ CITA National Fellow, Canadian Institute for Theoretical Astrophysics, University of Toronto, 60 Saint George Street, Toronto, Ontario M5S 1A7, Canada.

The difficulty arises in how the quarks interact. Free, isolated quarks are not seen experimentally, which implies that quarks are confined. If one tries to pull two quarks apart, the interaction between them gets stronger as the separation increases, not weaker as it would in electromagnetism (for comparison). This effect of increasing force with increasing separation can be modeled in a theory where there is more than one charge that a quark can carry. (In electromagnetism, there is only the one type of charge.) These distinct charges are called “color,” and we denote the number of colors by N_c . We have significant evidence now indicating that $N_c = 3$ provides a good representation of the strong interaction. In this theory, the force carrier is called a gluon (in electromagnetism it is the photon), and the gluons can actually carry color charge themselves. These are unusual properties that ultimately lead, we believe, to confinement.

Our attempts to understand the connection between QCD and nuclear physics rely, as mentioned earlier, on models and effective theories. One interesting approach was taken by 't Hooft (1974). He found that in the limit of a large number of colors (large N_c), $1/N_c$ could be used as an expansion parameter. In this limit, QCD simplifies a great deal, and 't Hooft went on to show that at large N_c , QCD is equivalent to a local field theory of mesons and “glueballs” (bound states of gluons, without quarks), with an effective interaction between them of order $1/N_c$.

The second step was taken by Witten (1979). Assuming confinement, he showed that baryons in large N_c QCD behave much like solitons in a weakly coupled local field theory of mesons. In this limit, baryon masses scale as $N_c = 1/g^2$, where g is the strength of the meson coupling, while baryon sizes are on the order of 1. Solitons in weakly coupled theories have masses that scale as $1/g^2$ and sizes that tend to constants as g tends to zero. Even though the mesons are weakly interacting, the solitons interact strongly, as do baryons in QCD.

At this time, it was realized that a model that incorporated these large N_c effects was already in existence. Skyrme (1962) constructed a model of pion interactions consisting of a conventional model of weak meson interactions plus an additional (higher order) term thought to take into account indirect effects of heavier mesons like the ρ meson. Skyrme found that his model contained “topologically nontrivial” configurations of the meson fields, namely, topological solitons, which Skyrme identified as baryons. *Note the similarities here to what Witten described as the nature of mesons and baryons in large N_c QCD.* Further study showed that while the mesons themselves were bosons, these topological solitons behaved as fermions (e.g., Witten 1983a, 1983b). Furthermore, topological solitons have a quantized topological charge, which could be identified as the baryon number B .

There are, of course, no guarantees that the Skyrme model is the correct representation of large N_c QCD. Furthermore, we can ask whether the large N_c limit is even relevant to the real world, where $N_c = 3$. Nonetheless, the connections are intriguing enough that the model warrants study on its predictions of hadronic interactions. Accordingly, in the last decade, there has been a large body of research on these solitons, or Skyrmions, especially by those interested in applying the Skyrme model to systems of many nucleons, aiming at the description of nuclei (Kälbermann 1997 and references therein).

These models belong to a class of effective models that treat the baryon stabilization (and hence the baryon structure) and the interaction between baryons on the same footing. There is no main difference between the stabilization and the interaction mechanism.

3. THE MEAN FIELD SKYRMION FLUID

In order to discuss a many-body system of Skyrmions, we follow the approach of Kälbermann (1997). In the so-called dilute fluid approximation, analogous to the mean field theory of pointlike baryons, one treats Skyrmions as essentially free particles interacting with a medium that carries the information of density and temperature.² The associated fields are the dilaton field, parameterized by σ , and the vector meson field ω . The dilaton field is associated with the glueball of QCD and originates from discussions of broken scale invariance (see Coleman 1985 for a discussion), while the vector meson field couples to the baryon number and helps maintain saturation in nuclear matter. Since the mass of the dilaton is large, we can neglect fluctuations in the dilaton field, even inside the Skyrmion.

In the approximation of a fluid of free Skyrmions, one demands that there is no overlap between the Skyrmion profile functions, and one further assumes that the profile drops to zero at a distance smaller than the inter-Skyrmion separation. These approximations ensure that the baryon number is quantized as an integer.

3.1. Properties of the Fluid

The Lagrangian for the Skyrmion in the presence of σ and ω fields is discussed, in detail, in Kälbermann (1997). We are concerned with the equations for the energy density and the mean field equations for ω and σ .

The association of σ with broken scale invariance means that one can show that it is only necessary to solve the equations of motion for a single free Skyrmion and then rescale the ω field and the radial distance by the simple scaling law

$$r \rightarrow e^{-\sigma_0} r, \quad \omega \rightarrow e^{-\sigma_0} \omega, \quad (1)$$

where $\sigma_0 = \langle \sigma \rangle$, the mean field value. Furthermore, the static mass scales as

$$M = M_0 e^{\sigma_0}, \quad (2)$$

where M_0 is the mass for $\sigma_0 = 0$, the mass of a single free Skyrmion.

At finite temperature, the energy of N Skyrmions per unit volume (parameterized by the density, ρ_V) in the mean field approximation is given by

$$E_V = 2g_N \int \frac{d^3p}{(2\pi)^3} E_p(n_p + \bar{n}_p) + V_\sigma(\sigma_0) - \frac{1}{2} e^{2\sigma_0} m_\omega^2 \omega_0^2 + g_V \omega_0 \rho_V \quad (3)$$

(in all of this section we adopt natural units with $\hbar = c = 1$), where $g_N = 1$ for neutron matter and $g_N = 2$ for symmetric

² Skyrmion-Skyrmion interactions are neglected, and consequently there are no potential terms depending on the coordinates of each baryon. There remains only the kinetic energy term for each individual Skyrmion.

nuclear matter representing the isospin degrees of freedom, and

$$E_p = \sqrt{p^2 + e^{2\sigma_0} M_0^2} \quad (4)$$

is the contribution to energy of a single Skyrmion; p is the Skyrmion's momentum, m_ω the vector meson mass, and

$$n_p = \left(\exp \frac{\epsilon_p - \mu}{kT} + 1 \right)^{-1}, \quad (5)$$

$$\bar{n}_p = \left(\exp \frac{\epsilon_p + \mu}{kT} + 1 \right)^{-1} \quad (6)$$

parameterize the single particle and antiparticle distribution functions with $\epsilon_p = E_p + g_V \omega_0$ and $\bar{\epsilon}_p = E_p - g_V \omega_0$. Here g_V is the strength of the coupling of the ω meson to baryons (Skyrmions), while

$$\rho_V = 2g_N \int \frac{d^3p}{(2\pi)^3} (n_p - \bar{n}_p). \quad (7)$$

In equation (3), V_σ is the dilaton potential, which we will discuss in § 3.2 when fitting parameters to the saturation properties of nuclear matter.

Here we further simplify our work by considering only $T = 0$ physics,³ that is, $n_p = \Theta(p_F - p)$ and $\bar{n}_p = 0$. Minimizing the energy density with respect to the mean field expectation values yields the equations of motion

$$0 = \frac{\partial E_V}{\partial \sigma_0} = 2g_N \int \frac{d^3p}{(2\pi)^3} \frac{\partial E_p}{\partial \sigma_0} + \frac{dV_\sigma}{d\sigma_0} - m_\omega^2 e^{2\sigma_0} \omega_0^2, \quad (8)$$

$$0 = \frac{\partial E_V}{\partial \omega_0} = m_\omega^2 e^{2\sigma_0} \omega_0 - g_V \frac{g_N p_F^3}{3\pi^2}, \quad (9)$$

with

$$p_F = \left(\frac{3}{g_N} \pi^2 \rho \right)^{1/3}, \quad (10)$$

the Fermi density simply obtained by integrating equation (7).

The pressure of such an ensemble at $T = 0$ is then given as

$$P_V = \rho_V^2 \frac{\partial (E_V/\rho_V)}{\partial \rho_V}. \quad (11)$$

The contribution of the vector meson field (ω) to the pressure grows with density ($\omega_0 \propto \rho_V$) and is positive; the dilaton potential $V(\sigma)$ gives a negative contribution to the pressure, acting to bind the system. As we show in § 3.3, these behaviors are crucial to understanding the behavior of the Skyrmion fluid at different nuclear densities.

3.2. Fitting Symmetric Nuclear Matter Properties

Once more following Kälbermann (1997), four free parameters (a_i and $i = 1, 4$) are added to the conventional dilaton potential, parameters that are required to reproduce

³ To a first approximation, the matter in neutron stars is in its ground state, its thermal energy is very small on the scale of typical excitation energies, and it may be assumed to be at $T = 0$.

nuclear matter phenomenology.⁴ It is

$$V_\sigma = B[1 + e^{4\sigma}(4\sigma - 1)] + B[a_1(e^{-\sigma} - 1) + a_2(e^\sigma - 1) + a_3(e^{2\sigma} - 1) + a_4(e^{3\sigma} - 1)], \quad (12)$$

with the ‘‘bag constant’’ $B \sim (240 \text{ MeV})^4$. Terms of the form $e^{n\sigma}$ are added to the potential to satisfy the anomaly condition, namely,

$$\frac{dV_\sigma}{d\sigma} = 0 \quad (13)$$

at $\sigma = 0$, implying $a_1 = a_2 + 2a_3 + 3a_4$.⁵ The parameters of the dilaton potential are constrained by demanding that at the saturation density of nuclear matter ($\rho_0 = 0.154$ baryons fm^{-3}), the properties of nuclear matter are recovered. For our purposes, we chose the effective mass $M^*/M_0 = M/M_0 = 0.6$, the compressibility $K = 270$ MeV, and a binding energy per nucleon ($M - E_V/\rho_V$) of 16 MeV.

On fitting to these properties, we find⁶

$$\begin{aligned} a_1 &= -1.69898, & a_2 &= -25.7806, \\ a_3 &= 29.2369, & a_4 &= -11.464, \end{aligned} \quad (14)$$

and

$$g_V = 7.54272. \quad (15)$$

Figure 1a shows the binding energy per nucleon as a function of the density. In all figures, the solid lines are for symmetric nuclear matter ($g_N = 1.0$), while the dotted lines are for pure neutron matter ($g_N = 2.0$). Figure 1b shows the Skyrmion effective mass (M^*) as a function of density. In the Walecka model, and many others similar to it, the nucleon effective mass decreases as a function of density. This is not the case in the Skyrmion fluid model. The minimum effective mass arises here at a density of around $1.2\rho_0$ for $g_N = 1.0$. The reason for this difference can be traced back to the dynamics dictated by the dilaton, especially to the modified trace anomaly potential, as explained in Kälbermann: the dilaton's attractive contribution to the mass is limited, while the ω meson repulsion grows in direct proportion to the nuclear matter density (eq. [9]). The solution of the nuclear matter equations then tends to push the dilaton toward positive values in order to fulfill the scaling properties of the model (eqs. [1]–[2]). This has serious consequences on the type of compact objects constructed and brings us to the discussion of the softness of our EOS.

3.3. Softness and Stiffness of the Skyrmion EOS

Figure 2a shows the pressure as a function of density for our EOS for the two cases of $g_N = 1$ (pure neutron matter; *solid line*) and $g_N = 2$ (symmetric matter; *dotted line*). Also shown is a sample of the EOS for symmetric nuclear matter described in the literature (Glendenning 1989; Weber &

⁴ There is also the possibility of modifying the ω field potential (see Kälbermann 1997 and references therein).

⁵ One chooses the term multiplied by a_1 to have a negative power of σ in order to avoid the introduction of a second minimum in the potential for $\sigma \leq 0$. The only sensible minimum, then, remains the one at $\sigma = 0$.

⁶ We note that these results differ substantially from those of Kälbermann 1997. However, there are a number of typographical errors in that paper concerning the equations for the properties of saturated nuclear matter, making it difficult to compare our results with his.

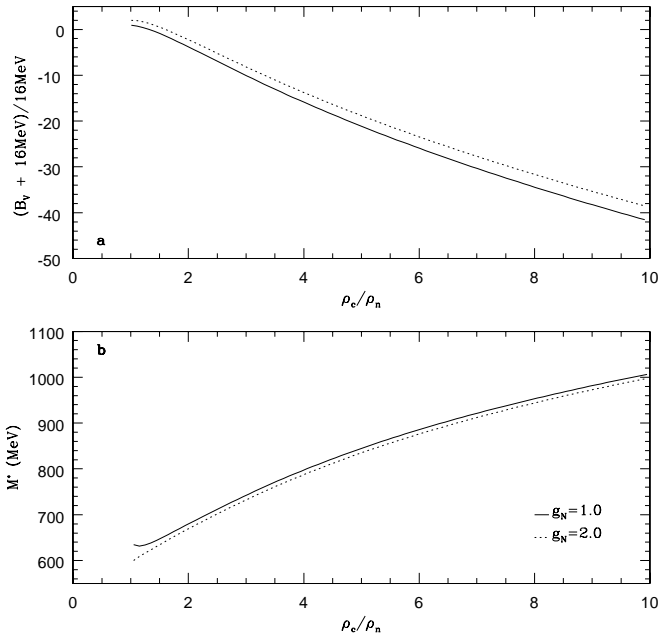


FIG. 1.—(a) Binding energy per nucleon, as a function of the central density. In all figures, the solid line is for pure neutron matter ($g_N = 1.0$), while the dotted line is for symmetric nuclear matter ($g_N = 2.0$). (b) Effective Skyrion mass M^* as a function of density for $T = 0$.

Weigel 1989; Baldo et al. 1997; Prakash et al. 1997; Shen et al. 1998). All EOSs have been fitted to reproduce nuclear matter parameters at saturation density.

Note that for high densities, our pressure is the highest; our EOS is the *stiffest* one. One would expect it, then, to construct compact objects that are even more massive than those constructed using the standard EOS, like those in

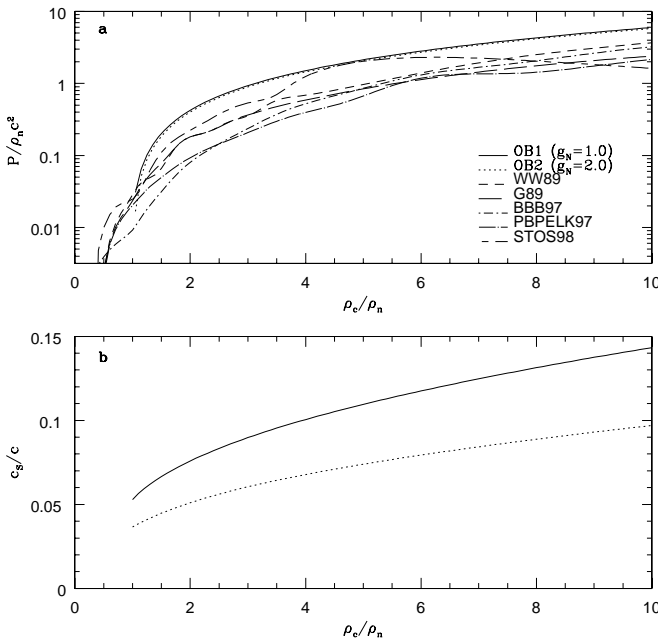


FIG. 2.—(a) Pressure as a function of the central density for $T = 0$ in our model, as compared with a sample of four symmetric matter EOSs (Glendenning 1989; Weber & Weigel 1989; Baldo et al. 1997; Prakash et al. 1997; Shen et al. 1998). Our EOS is plotted for the two cases of $g_N = 1.0$ (pure neutron matter) and $g_N = 2.0$ (symmetric matter). (b) Speed of sound as a function of density. The causality condition is not violated.

Figure 2. However, this is not the case here. It was mentioned in § 3.2 that the nucleon effective mass increases above a certain density. This is a result of a decrease in the magnitude of the mean dilaton field σ_0 . The scaling relations of equation (1) would then also imply that the Skyrion begins to shrink. This is reminiscent of the behavior of the Skyrion interaction at short range (high density) that is known to be repulsive and strong. This peculiarity allows for exotic behavior of matter at high densities (there will be more on this in § 5).

3.4. Causality

Finally, special relativity requires that the sound velocity in dense matter be not larger than c . At $T = 0$, this is equivalent to

$$\frac{dP}{d\rho} < 1. \quad (16)$$

Figure 2b clearly shows that our EOS does not violate the causality condition.

4. NONROTATING SKYRMION STARS

We proceed now to construct models for nonrotating stars using the EOS developed above. This is done by integrating the general relativistic equation of hydrostatic balance

$$\frac{dP(r)}{dr} = -\frac{G[\rho(r) + P(r)/c^2][m(r) + 4\pi r^3 P(r)/c^2]}{r^2[1 - 2Gm(r)/rc^2]}, \quad (17)$$

$$\frac{dm(r)}{dr} = 4\pi r^2 \rho(r) \quad (18)$$

(Tolman 1934; Oppenheimer & Volkov 1939), where G is the gravitational constant, P is the pressure, ρ is the density, and $m(r)$ the enclosed gravitational mass. The gravitational mass of the star is then given by

$$M_G = \int_0^R dr 4\pi r^2 \rho(r), \quad (19)$$

while the total baryon number is

$$B = \int_0^R dr 4\pi r^2 \frac{n(r)}{[1 - 2Gm(r)/rc^2]^{1/2}}. \quad (20)$$

Here $n(r)$ is the baryon number density,

$$n(r) = \frac{\rho(r)}{m_A - B_N}, \quad (21)$$

where m_A is the baryonic mass and B_N is the (nuclear) binding energy per nucleon. The baryon mass of the star becomes $M_A = m_A B$, with the total binding energy of the star defined as B.E. = $(M_A - M_G)c^2$. The radius of the star is determined by

$$P(R) = 0. \quad (22)$$

Introducing the new variables

$$r = R_{\text{Sc}, \odot} \bar{r}, \quad m = M_{\odot} \bar{m}, \quad \rho = \rho_N \bar{\rho}, \quad p = \rho_N c^2 \bar{p}, \quad (23)$$

where M_{\odot} is the solar mass, $R_{\text{Sc}, \odot} = 2GM_{\odot}/c^2$, the Sun's Schwarzschild radius, and $\rho_N = 0.154$ baryons fm^{-3} , the nuclear saturation density, equations (17) and (18), are

rewritten as

$$\frac{d\bar{P}(\bar{r})}{d\bar{r}} = -\frac{1}{2} \frac{[\bar{\rho}(\bar{r}) + \bar{P}(\bar{r})][\bar{m}(\bar{r}) + \zeta\bar{r}^3\bar{P}(\bar{r})]}{\bar{r}^2[1 - \bar{m}(\bar{r})/\bar{r}]}, \quad (24)$$

$$\frac{d\bar{m}(\bar{r})}{d\bar{r}} = \zeta\bar{r}^2\bar{\rho}(\bar{r}), \quad (25)$$

with $\zeta = 4\pi R_{\text{Sc},\odot}^3 \rho_N / M_\odot$. From now on, for simplicity, we drop the bars, keeping in mind that our quantities henceforth represent dimensionless variables.

Equations (24) and (25) are readily integrated numerically for our given EOS to construct the pressure profile $P(r)$ and, from this, the mass density profile $\rho(r)$. The single integration constant P_c , the pressure at the center of the star, completely specifies the solution. The actual numerical integration was done by a five-point Runge-Kutta sequence. Each integration step yields a value of $P(r)$, and the value of $\rho(r)$ was constructed from the numerical EOS by interpolating ρ as functions of P . Note that in our model, equations (8) and (9) (mean field equations) must be used at each time step to interpolate σ and ω as a function of ρ .

4.1. Crust Region

For ease of computation, we have adopted the sub-nuclear EOS of Baym, Pethick, & Sutherland (1971, hereafter BPS) for all the hydrostatic models we have built. The crustal mass (defined as the matter exterior to the uniform

fluid of neutrons, protons, and electrons)⁷ depends strongly on the density at which the transition to the uniform fluid phase occurs. Lorenz, Ravenhall, & Pethick (1993), for example, found that the transition (where nuclei disappear and the matter becomes uniform) occurs at about $0.6\rho_N$. They concluded that the mass of matter in the crust is only half as large as previously estimated, on the assumption that nuclei dissolve at approximately nuclear matter density, as found by BPS. However, the choice of the EOS in this regime is of little consequence to our work/conclusion. We do, however, refer the interested reader to Pethick & Ravenhall (1995) for the key role played by the crust in the study of the evolution of the neutron stars.

4.2. Comparison with Observations

While constructing Skymion stars, we keep in mind the constraints on the EOS inferred by observations of neutron stars.

4.2.1. Mass

Figure 3a shows the resulting stellar masses as a function of the central density. The maximum-mass (minimum-mass) Skymion star is $2.9 M_\odot$ ($0.5 M_\odot$) for symmetric nuclear matter ($g_N = 2.0$) and $2.95 M_\odot$ ($0.7 M_\odot$) for pure neutron matter ($g_N = 1.0$). Our maximum mass M_{max} exceeds the

⁷ See BPS for the details of the constituents of the crust.

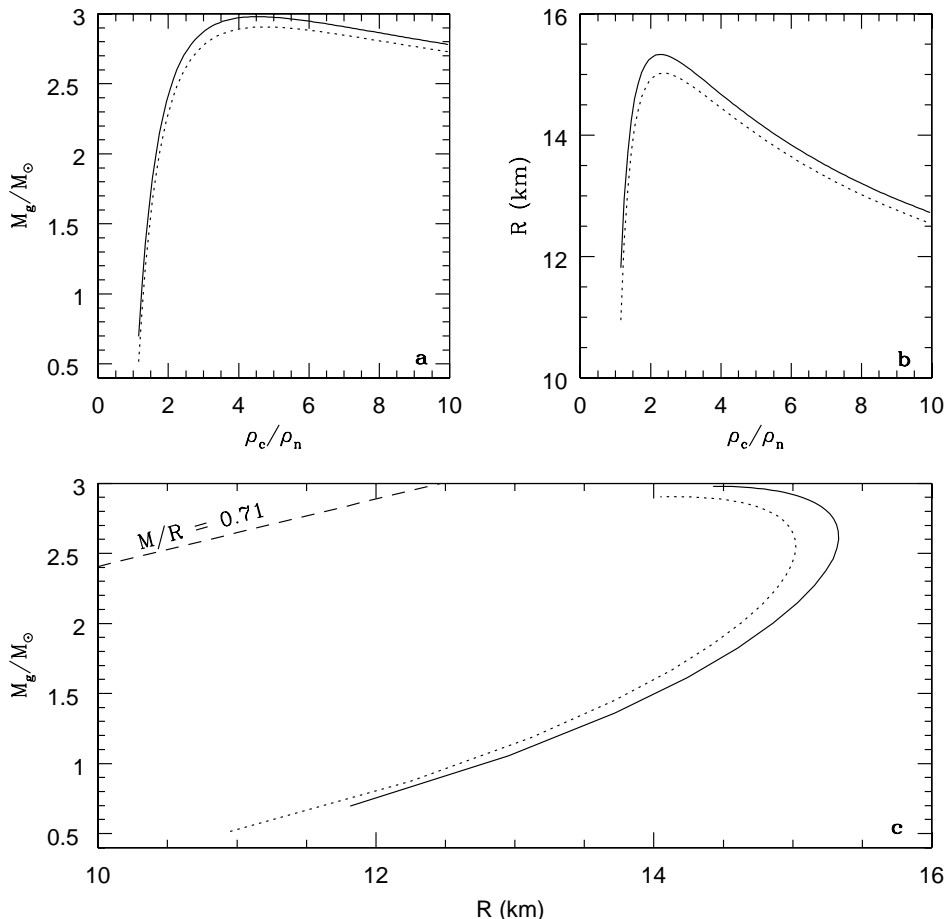


FIG. 3.—(a) Mass vs. central density for zero-temperature nonrotating Skymion stars in hydrostatic equilibrium. (b) Radius vs. central density for zero-temperature nonrotating Skymion stars in hydrostatic equilibrium. (c) The mass-radius plane. The dashed line corresponds to the upper bound for the surface redshift of neutron stars with causal EOSs; $M/R \leq 0.71$ (see § 4.2.3).

largest of the observed neutron star masses; that is, $M_{\max} \geq 1.44 M_{\odot}$, as it should. Stars with central densities $\rho \leq \rho_c$ (where $\rho_c = 4.5$ for symmetric nuclear matter, $g_N = 2.0$ and $\rho_c = 5.0$ for pure neutron matter, and $g_N = 1.0$) represent stable Skyrmion stars, while configurations with central densities $\rho \geq \rho_c(M_{\max})$ are unstable toward small perturbations and are thought to form black holes.

4.2.2. Radius

Figure 3b shows the resulting stellar radii as a function of the central density. The range of radii is $11.0 \text{ km} \leq R \leq 15.0 \text{ km}$ for symmetric nuclear matter and $11.8 \text{ km} \leq R \leq 15.3 \text{ km}$ for pure neutron matter. Until recently, direct radius determinations for neutron stars were nonexistent. Walter & Matthews (1997), with the discovery of the optical counterpart of *isolated* neutron stars, were able to infer an upper limit on the object radius. They estimate $R_{\max} = 14(D/130) \text{ km}$, based on the fact that the upper limit to the distance to the object ($D \leq 130 \text{ pc}$) is reasonably certain (although the true distance to the isolated neutron star is still unknown). The size of our constructed objects are in good agreement with these observations for as long as $D \geq 90 \text{ pc}$, a notion still to be confirmed.

4.2.3. The Mass-Radius Plane

Figure 3c represents the mass-radius plane for the Skyrmion stars constructed here. In this figure and in the rest of the figures, only stable configurations with $\rho \leq \rho_c$ (or $M \leq M_{\max}$) are shown. Configurations with a mass higher than M_{\max} can be shown to be unstable with respect to small radial perturbations—and therefore could not exist in the universe. The dashed line corresponds to the upper bound for the surface redshift of neutron stars with causal EOS, $z_{s,\max} = 0.85$, calculated by Lindblom (1984). The region in the M - R plane allowed by the general theory of relativity and causality thus corresponds, according to Lindblom, to $M/R \leq 0.71$.

4.2.4. Binding Energy

Estimates of the energy released in neutrinos from the SN 1987A explosion places a restriction on the EOS that the B.E. $\geq (2-4) \times 10^{53} \text{ ergs}$ or B.E. $\geq (0.1-0.3) M_{\odot} c^2$ (Burrows & Lattimer 1986, for example). Nearly all (up to 99%) of the binding energy of a neutron star is released in the form of neutrinos during the birth of a neutron star. The computed total binding energy for the Skyrmion stars constructed here (Fig. 4a) show no disagreement with observations. The total number of baryons is shown in Figure 4b.

4.2.5. Gravitational Redshift

Figure 4c shows the gravitational redshift of photons emitted radially from the Skyrmion star surface with wavelength λ_s , which will be detected far from the star with wavelength λ_{∞} :

$$z_s = \frac{\lambda_{\infty} - \lambda_s}{\lambda_s} = \left(1 - \frac{M}{R}\right)^{-1/2} - 1. \quad (26)$$

The value of z_s can be determined by measuring the redshift of a given emission or absorption line in the spectrum of the surface radiation of the object.

To complete this section, Figure 5a shows the density profile for a $1 M_{\odot}$ and a $2 M_{\odot}$ model for symmetric matter (*dotted line*) and for pure neutron matter (*solid line*). Figure 5b shows the amount of mass in the outer region of the star:

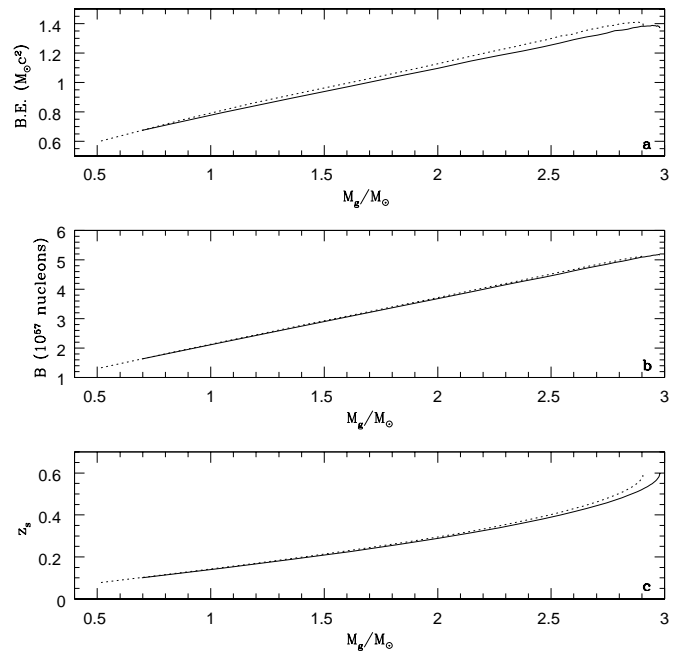


FIG. 4.—(a) Binding energy vs. gravitational mass. (b) Total number of nucleons vs. gravitational mass. (c) Gravitational redshift vs. gravitational mass.

the crust region (constructed using the EOS of BPS; see § 4.1). On average, more than 80% of the mass in the stellar interior has density $\rho > \rho_N$ and constitutes the dense Skyrmion fluid interior.

5. DISCUSSION AND CONCLUSION

In this work, we have considered a new EOS of dense matter based on a fluid of Skyrmions coupled to the dilaton field and the ω meson. Our interest in such a model is the

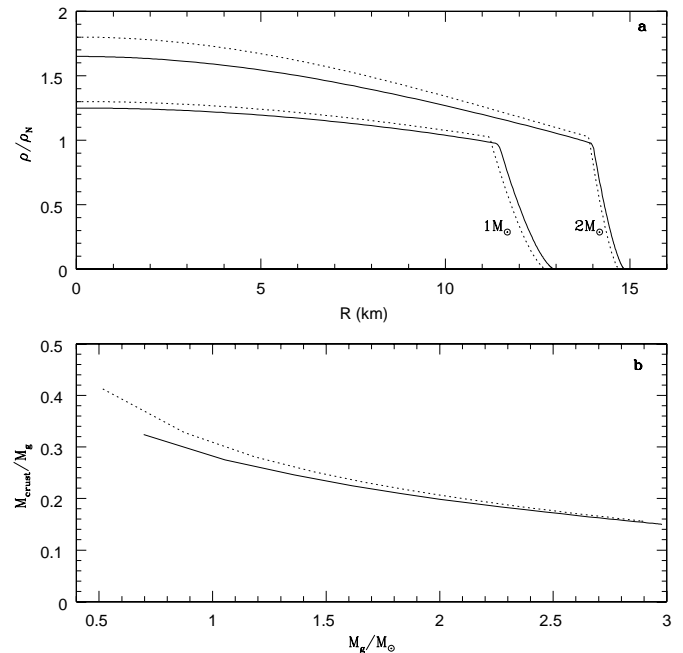


FIG. 5.—(a) Density profiles for 1 and $2 M_{\odot}$ models of Skyrmion stars. (b) Crustal mass fraction. The crust is defined as the subnuclear region where the EOS of BPS has been adopted (see the discussion in § 4.1).

consequence of its recent revival and its plausible link to low-energy QCD. Most importantly, the Skyrmion fluid model is mathematically more tractable than QCD. We have constructed zero-temperature compact-star models in hydrostatic equilibrium. We found stable configurations to exist for central densities $\rho_c/\rho_N \leq 5.0$. Their masses and radii are $0.5 \leq M/M_\odot \leq 2.95$ and $11.0 \text{ km} \leq R \leq 15.3 \text{ km}$, respectively. In our model, we predict the heaviest Skyrmion stars to rotate the fastest (Ouyed & Butler 1999). This is the result of the shrinkage of the Skyrmons as the density increases, allowing for high central compression of matter near the core of the star and thus greater gravitational binding energy. Much of this interesting behavior arises from the nature of the dilaton field, whose attractive contribution to the mass is limited, unlike the ω meson repulsive contribution, which grows in direct proportion to the density. In fact, this behavior of the dilaton field does not necessarily arise only in models of Skyrmons but could be studied elsewhere.

5.1. Skyrmons Stars and “Exotic” Stars

While Skyrmon stars form their constituent baryons as topological solitons using pion (boson) fields, they are not boson/soliton stars (e.g., Jetzer 1992; Lee & Pang 1992), where the soliton is a global structure over the scale of the star. Skyrmon stars, however, could be looked at in the context of fermion soliton stars (Lee & Pang 1987) or fermion Q stars (Bahcall, Lynn, & Selipsky 1989). In these models, pointlike fermions interact with scalar boson fields, which have a topological structure. These do not, however, demonstrate the rescaling properties that we see in Skyrmon stars at high densities because of the dilaton field, a result of Skyrmons having structure. Furthermore, we should also note that Skyrmon stars are *not* quark stars (Haensel, Zdunik, & Schaeffer 1986; Alcock, Farhi, & Olinto 1986). While the Skyrme model might be a representation of QCD at large N_c , the quark degrees of freedom are integrated out, and mesons are the fundamental degrees of freedom.

5.2. Quantum Skyrmion

The classical treatment of the Skyrmon is still questionable. For example, the static soliton solutions can be shown to be unstable against radial collapse because of the Derrick instability (Derrick 1964); the energy collapses to zero as the Skyrmon shrinks (note that in our treatment of the Skyrmon fluid, the ω meson provides additional terms to the Lagrangian, which then gives stable Skyrmons). However, it has been shown that the Skyrmon is stable if its radial extent and its orientation in space are treated as quantum variables (Abdalla & Preston 1996 and references therein).⁸ One other problem that arises as a consequence of the classical approach is the absence of a distinction between neutron and proton interactions. Further study would be required for the fully quantized Skyrme model, so that neutron and proton interactions are distinguished and a symmetry energy can arise.

In the end, despite the fact that there are no guarantees that our model is a correct representation of nuclear matter, it is surprisingly successful in reproducing most of the properties of observed compact stars. This might be an indication that it warrants more detailed study.

R. O. acknowledges the financial support of the Department of Astronomy and Physics, Saint Mary’s University, Halifax, Canada, and the Canadian Institute for Theoretical Astrophysics, Toronto, Canada. R. O. is grateful to A. H. Abdalla, R. K. Bhaduri, M. A. Preston, and D. W. L. Sprung for all the help provided during the course of this work. M. B. is supported by a grant from the Natural Science and Engineering Research Council of Canada. We are grateful to an anonymous referee for the remarks that helped improve this work.

⁸ Taking account of these features gives a good value of the axial coupling constant that controls the neutron lifetime (A. H. Abdalla & M. A. Preston 1999, private communication).

REFERENCES

- Abdalla, A. H., & Preston, M. A. 1996, *Phys. Rev. D*, 53, 3967
 Akmal, A., Pandharipande, V. R., & Ravenhall, D. G. 1998, *Phys. Rev. C*, 58, 1804
 Alcock, C., Farhi, E., & Olinto, A. 1986, *ApJ*, 310, 261
 Bahcall, S., Lynn, B. W., & Selipsky, S. B. 1989, *Nucl. Phys. B*, 325, 606
 Baldo, M., Bombaci, I., & Burgio, G. F. 1997, *A&A*, 328, 274
 Baym, G., Pethick, C. J., & Sutherland, P. G. 1971, *ApJ*, 170, 299 (BPS)
 Bhaduri, R. K. 1988, *Models of the Nucleon: from Quarks to Soliton* (Redwood City: Addison Wesley)
 Brown, G. E., & Bethe, H. A. 1994, *ApJ*, 423, 659
 Burrows, A., & Lattimer, J. M. 1986, *ApJ*, 307, 178
 Coleman, S. 1985, *Aspects of Symmetry: Selected Erice Lectures* (Cambridge: Cambridge Univ. Press)
 Derrick, G. H. 1964, *J. Math. Phys.*, 5, 1252
 Glendenning, N. K. 1989, *Nucl. Phys. A*, 493, 521
 Haensel, P., Zdunik, J. L., & Schaeffer, R. 1986, *A&A*, 160, 121
 Jetzer, P. 1992, *Phys. Rep.*, 220, 163
 Kälbermann, G. 1997, *Nucl. Phys. A*, 612, 359
 Lattimer, J. M., & Swesty, D. F. 1991, *Nucl. Phys. A*, 535, 331
 Lee, T. D., & Pang, Y. 1987, *Phys. Rev. D*, 35, 3678
 Lee, T. D., & Pang, Y. 1992, *Phys. Rep.*, 221, 251
 Lindblom, L. 1984, *ApJ*, 278, 364
 Lorenz, C. P., Ravenhall, D. G., & Pethick, C. J. 1993, *Phys. Rev. Lett.*, 70, 379
 Oppenheimer, J. R., & Volkoff, G. M. 1939, *Phys. Rev.*, 55, 374
 Ouyed, R., & Butler, M. 1999, in preparation
 Pethick, C. J., & Ravenhall, D. G. 1995, *Annu. Rev. Nucl. Part. Sci.*, 45, 54
 Prakash, M., Bombaci, I., Prakash, M., Ellis, P. J., Lattimer, J. M., & Knorren, R. 1997, *Phys. Rep.*, 280, 1
 Shen, H., Toki, H., Oyamatsu, K., & Sumiyoshi, K. 1998, *Nucl. Phys. A*, 657, 435
 Skyrme, T. H. R. 1962, *Proc. R. Soc. London A*, 260, 127
 ’t Hooft, G. 1974, *Nucl. Phys. B*, 72, 461
 Tolman, R. C. 1934, *Proc. Natl. Acad. Sci.*, 20
 Walter, F. M., & Matthews, L. D. 1997, *Nature*, 389, 358
 Weber, F., & Weigel, M. K. 1989, *Nucl. Phys. A*, 505, 779
 Witten, E. 1979, *Nucl. Phys. B*, 160, 57
 ———. 1983a, *Nucl. Phys. B*, 223, 422
 ———. 1983b, *Nucl. Phys. B*, 223, 443